INSTITUTE OF PHYSICS PUBLISHING NONLINEARITY

Nonlinearity **18** (2005) 2827–2846 doi:10.1088/0951-7715/18/6/022

# Equivariant Hopf bifurcation in a ring of identical cells with delayed coupling

**Sue Ann Campbell**[1,2], **Yuan Yuan**[3] **and Sharene D Bungay**[1,4]

[1] Department of Applied Mathematics, University of Waterloo, Waterloo, ON, N2L 3G1, Canada
[2] Centre for Nonlinear Dynamics in Physiology and Medicine, McGill University, Montréal, QC, H3G 1Y6, Canada
[3] Department of Mathematics and Statistics, Memorial University of Newfoundland, St. John's, Newfoundland, A1C 5S7, Canada

E-mail: sacampbell@uwaterloo.ca

Received 21 June 2005, in final form 7 September 2005
Published 7 October 2005
Online at stacks.iop.org/Non/18/2827

Recommended by D Treschev

**Abstract**
We consider a ring of identical elements with time delayed, nearest-neighbour coupling. The individual elements are modelled by a scalar delay differential equation which includes linear decay and nonlinear delayed feedback. The bifurcation and stability of nontrivial asynchronous oscillations from the trivial solution are analysed using equivariant bifurcation theory and centre manifold construction.

Mathematics Subject Classification: 34K17, 37G40, 92B20

## 1. Introduction

The work of Golubitsky *et al* [12] shows that systems with symmetry can lead to many interesting patterns of oscillation, which are predictable based on the theory of equivariant bifurcations. In a series of papers, Wu and co-workers [20, 21, 29] extended the theory of equivariant Hopf bifurcation to systems with time delays (functional differential equations). It should be noted that this theory predicts the *possible* patterns of oscillation in a system solely on the symmetry structure of the system. To understand which patterns occur in a particular system and whether they are stable, one needs to consider a specific model for a system.

With this in mind, there has been interest in applying these results to models related to the Hopfield–Cohen–Grossberg neural networks [8, 13, 14, 18, 19] with time delays [22, 24]. Such models make an ideal test bed for this theory as the models for the individual elements

[4] Current address: Department of Computer Science, Memorial University of Newfoundland, St John's, Newfoundland, A1C 5S7, Canada.

  

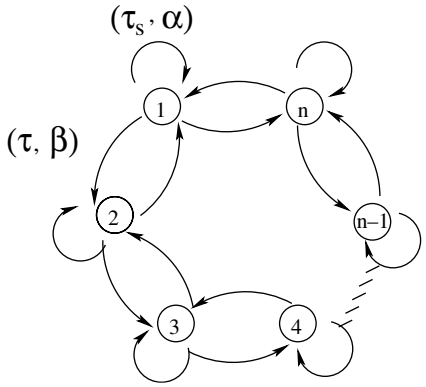


**Figure 1.** Architecture of a network of $n$ neurons with two different time delays. $\tau_s$, $\alpha$ are the time delay and strength of the connection of each element to itself. $\tau$, $\beta$ are the time delay and strength of the connections between different elements.

are quite simple (one variable for each element), yet with the introduction of time delays the behaviour can be quite complex. The focus of this work has been on networks with a ring structure with nearest-neighbour (bi-directional) coupling between the elements. This leads to a system with $\boldsymbol{D}_n$ symmetry, i.e. a system which has the symmetries of a polygon with $n$ sides of equal length. Most of these studies have concerned lower dimensional systems (e.g. [6,25,30]) and/or systems with a single time delay [16, 29, 30]. There is also work on Hopfield–Cohen–Grossberg networks with a ring structure and uni-directional coupling [1,5,7,28]. These studies did not consider identical elements, however, and thus did not use the theory of equivariant bifurcations.

Other work on systems with symmetry and time delays includes that of Orosz and Stépán [26], who studied a quite general system with translational symmetry and one time delay using centre manifold and normal form analysis. They applied their results to a two-dimensional car following model with periodic boundary conditions, which leads to a system with a ring structure and uni-directional coupling. Orosz *et al* [27] studied the $n$-dimensional version of this model using local bifurcation theory and numerical continuation analysis.

Here we will consider a Hopfield–Cohen–Grossberg network consisting of $n$ identical elements with time delayed nearest-neighbour coupling, as illustrated schematically in figure 1. The individual elements are represented by a scalar equation, consisting of a linear decay term and a nonlinear, time delayed self-connection (feedback) giving the following model of the network:

$$\dot{x}_i(t) = -x_i(t) + \alpha f(x_i(t-\tau_s)) + \beta\,[g(x_{i-1}(t-\tau)) + g(x_{i+1}(t-\tau))], \qquad i \,(\mathrm{mod}\ n). \tag{1}$$

Here $\tau$ represents the time delay in the connections between different elements and $\tau_s$ the time delay in the self-connection. This is a generalization to arbitrary $n$ of the model of [6,25]. The main difference from the model considered by [16, 29] is that there are different time delays in the self-connections and the connections between elements. This adds some complications to the analysis but, as we shall show, also allows for more interesting behaviour of the system. In [31] we analysed the linear stability of the trivial solution of (1) and the bifurcation and stability of nontrivial synchronous solutions from the trivial solution. In order to describe the existence and stability of asynchronous patterns of oscillation in this network, we must consider the points of equivariant Hopf bifurcation. This is the goal of this work.

To begin, we give some assumptions and background about our model. We will assume that the nonlinearities $f, g$ are adequately smooth, e.g. $f, g \in C^3$, satisfy the following normalization conditions:

$$f(0) = g(0) = 0, \qquad f'(0) = g'(0) = 1, \qquad f''(0) = g''(0) = 0 \tag{2}$$

and satisfy at least one of the following nondegeneracy conditions:

$$f'''(0) \neq 0, \qquad g'''(0) \neq 0. \tag{3}$$

An example of such a function is $(1/\gamma)\tanh(\gamma x)$, which we will use for our numerical studies. The delays will be taken to be nonnegative, $\tau, \tau_s \geqslant 0$, but the connection strengths have no sign restriction. Positive/negative connection strengths correspond to excitatory/inhibitory connections. We note that when $n = 2$, the model is not in the 'natural' setup; however, it can be transformed to this by rescaling $2\beta$ to $\beta$.

When isolated, each of the individual elements of equation (1) satisfies the scalar delay differential equation

$$\dot{x}_i(t) = -x_i(t) + \alpha f(x_i(t - \tau_s)). \tag{4}$$

It is well known (see, e.g. [5]) that for $f$ satisfying conditions such as (2), the trivial solution always exists and is locally asymptotically stable if

$$\begin{aligned} &-1 \leqslant \alpha < 1 \quad \text{and} \quad \tau_s \geqslant 0, \\ &\alpha < -1 \quad \text{and} \quad 0 \leqslant \tau_s < \frac{1}{\sqrt{\alpha^2 - 1}} \operatorname{Arccos}\left(\frac{1}{\alpha}\right) \stackrel{\text{def}}{=} \tau_s^H \end{aligned} \tag{5}$$

and unstable if

$$\begin{aligned} &\alpha > 1 \quad \text{and} \quad \tau_s \geqslant 0, \\ &\alpha < -1 \quad \text{and} \quad \tau_s > \tau_s^H. \end{aligned} \tag{6}$$

Further, there is a steady state bifurcation at $\alpha = 1$ and a Hopf bifurcation at $\tau = \tau_s^H$ when $\alpha < -1$. We can thus consider our model as a ring of $n$ identical coupled oscillators with time delayed, nearest-neighbour coupling. This makes it a natural extension to systems with time delay of the work of Golubitsky *et al* [12, chapter XVIII] on rings of coupled oscillators. In particular, since we have different time delays in the self-connections and those between elements, we can focus on the oscillations produced by the network parameters $\tau$ and $\beta$.

The outline of this paper is as follows. In section 2 we briefly review some relevant results from our previous work [31] and some background and notation from the theory of delay differential equations and equivariant bifurcations. In section 3 we describe the existence of asynchronous oscillations in our system via an equivariant Hopf bifurcation theorem. In section 4 we study the criticality and stability of these solutions using a centre manifold construction. In section 5 we compare our theoretical results with those from numerical continuation for a particular example. Finally, in section 6 we discuss the implications of our results.

## 2. Preliminaries

From conditions (2) it is clear that (1) admits the trivial solution, $x^* = 0$, and that the linearization of (1) at this equilibrium point is

$$\dot{u}_i(t) = -u_i(t) + \alpha u_i(t - \tau_s) + \beta[u_{i-1}(t - \tau) + u_{i+1}(t - \tau)] \qquad i \,(\text{mod } n). \tag{7}$$

In vector form, this can be written as

$$\dot{\boldsymbol{u}}(t) = -I\boldsymbol{u}(t) + \alpha I\boldsymbol{u}(t - \tau_s) + \beta M\boldsymbol{u}(t - \tau), \tag{8}$$

where $I$ is the $n \times n$ identity matrix and

$$M = \begin{pmatrix} 0 & 1 & 0 & \cdots & 1 \\ 1 & 0 & 1 & \cdots & 0 \\ 0 & 1 & 0 & \cdots & 0 \\ \vdots & \vdots & \vdots & \cdots & \vdots \\ 1 & 0 & 0 & \cdots & 0 \end{pmatrix}_{n\times n}. \tag{9}$$

Thus the characteristic matrix of the linearization of (1) about the trivial solution is

$$\mathcal{M}_n(\lambda) = (\lambda + 1 - \alpha e^{-\lambda\tau_s})I - \beta e^{-\lambda\tau} M \tag{10}$$

and the corresponding characteristic equation is

$$\det \mathcal{M}_n(\lambda) = 0. \tag{11}$$

It can be shown [31] that

$$\begin{aligned} \det \mathcal{M}_n(\lambda) &= \prod_{k=0}^{n-1} \Delta_k(\lambda) \\ &= \begin{cases} \Delta_0(\lambda) \displaystyle\prod_{k=1}^{(n-1)/2} \Delta_k^2(\lambda) & (\text{if } n \text{ is odd}), \\ \Delta_0(\lambda)\Delta_{n/2}(\lambda) \displaystyle\prod_{k=1}^{(n/2)-1} \Delta_k^2(\lambda) & (\text{if } n \text{ is even}), \end{cases} \end{aligned} \tag{12}$$

where $\Delta_k(\lambda) = \lambda + 1 - \alpha e^{-\lambda\tau_s} - 2\beta e^{-\lambda\tau}\cos(2\pi k/n)$.

From (12), it is clear that the characteristic equation has a repeated pair of pure imaginary roots $\lambda = \pm i\omega$ for parameters such that $\Delta_j(\pm i\omega) = 0$, for some $j \in \{1, 2, \ldots, [(n-1)/2]\}$, $j \neq n/4$, i.e. when

$$\begin{aligned} 1 - \alpha\cos(\omega\tau_s) &= 2\beta\cos\left(\frac{2\pi j}{n}\right)\cos(\omega\tau), \\ \omega + \alpha\sin(\omega\tau_s) &= -2\beta\cos\left(\frac{2\pi j}{n}\right)\sin(\omega\tau). \end{aligned} \tag{13}$$

In particular, if we fix three of the parameters, this gives two equations that may be solved for the critical value of the fourth parameter and the corresponding imaginary part of the eigenvalue, $\omega_c$. Here we will focus on using network connection strength, $\beta$, as the bifurcation parameter. In fact all the results hold (and are proved similarly) if any of the other parameters is used instead.

Taking the ratio of the two equations of (13) yields an implicit equation for $\omega_c$:

$$\tan(\omega_c\tau) + \frac{\omega_c + \alpha\sin(\omega_c\tau_s)}{1 - \alpha\cos(\omega_c\tau_s)} = 0. \tag{14}$$

Squaring and adding the equations of (13) yields an equation for the corresponding critical value of $\beta$ (for the $j$th factor of the characteristic equation):

$$\beta_{cj}(\omega_c) = \begin{cases} \hat{\beta}_{cj}(\omega_c) & \text{if } (1 - \alpha\cos(\omega_c\tau_s))\cos\left(\dfrac{2\pi j}{n}\right)\cos(\omega_c\tau) > 0, \\ -\hat{\beta}_{cj}(\omega_c) & \text{if } (1 - \alpha\cos(\omega_c\tau_s))\cos\left(\dfrac{2\pi j}{n}\right)\cos(\omega_c\tau) < 0, \end{cases} \tag{15}$$

where

$$\hat{\beta}_{cj}(\omega_c) = \frac{1}{2|\cos(2\pi j/n)|}\sqrt{1+\alpha^2+\omega_c^2+2\alpha\omega_c\sin(\omega_c\tau_s)-2\alpha\cos(\omega_c\tau_s)}.$$

In [31] we give a complete characterization of when solutions to these equations exist.

To carry out our work we need some background from the theory of functional differential equations. Let $h = \max(\tau_s, \tau)$ and $\mathcal{C} \stackrel{\text{def}}{=} C([-h, 0], \mathbb{R}^n)$ denote the Banach space of continuous mappings from $[-h, 0]$ into $\mathbb{R}^n$ equipped with the supremum norm $\|\phi\|_h = \sup_{-h\leqslant\theta\leqslant 0}\|\phi(\theta)\|$ where $\|\cdot\|$ is the usual Euclidean norm on $\mathbb{R}^n$. Let $x(t)$ be a solution of (1) and define $x_t(\theta) = x(t+\theta)$, $-h \leqslant \theta \leqslant 0$. If $x(t)$ is continuous, then $x_t(\theta) \in \mathcal{C}$. With this structure, we may write the model as the following *functional differential equation*:

$$\dot{\boldsymbol{x}}(t) = \boldsymbol{F}(\boldsymbol{x}_t), \tag{16}$$

where $\boldsymbol{F} : \mathcal{C} \to \mathbb{R}^n$ is defined via

$$F_i(\phi) = -\phi_i(0) + \alpha f(\phi_i(-\tau_s)) + \beta[g(\phi_{i-1}(-\tau)) + g(\phi_{i+1}(-\tau))], \qquad i \,(\text{mod } n). \tag{17}$$

Similarly, the linearized equation (8) may be written as

$$\dot{\boldsymbol{u}}(t) = L(\beta)\boldsymbol{u}_t, \tag{18}$$

where the linear operator $L(\beta) : \mathcal{C} \to \mathbb{R}^n$ is defined via

$$L(\beta)\phi = -I\phi(0) + \alpha I\phi(-\tau_s) + \beta M\phi(-\tau). \tag{19}$$

It is well known [17] that a linear functional differential equation such as (18) generates a strongly continuous semigroup of linear operators with infinitesimal generator $A(\beta)$ given by

$$\begin{aligned} &A(\beta)\phi = \dot{\phi}, \qquad \phi \in \text{Dom}(A), \\ &\text{Dom}(A) = \{\phi \in \mathcal{C} | \dot{\phi} \in \mathcal{C}, \dot{\phi}(0) = L(\beta)\phi\}. \end{aligned} \tag{20}$$

Further, the eigenvalues of $A(\beta)$ correspond to the roots of the characteristic equation (11).

Finally, to discuss the spatial symmetry of (1) we need some notation from the theory of compact groups.

- $\boldsymbol{Z}_n$ is the cyclic group of order $n$, which corresponds to rotations of $2\pi/n$. Denoting the generator of this group by $\rho$, then its action on $\mathbb{R}^n$ is given by $(\rho x)_i = x_{i+1}$.
- Let $\kappa$ be the flip of order 2 or reflection. It acts on $\mathbb{R}^n$ by $(\kappa x)_i = x_{n+2-i}$.
- $\boldsymbol{D}_n$ is the dihedral group of order $n$, which corresponds to the group of symmetries of an $n$-gon. It can be shown that $\boldsymbol{D}_n$ is generated by $\rho$ and $\kappa$.

**Definition.** Let $\boldsymbol{F} : \mathcal{C} \to \mathbb{R}^n$ and $\Gamma$ be a compact group. The system $\dot{\boldsymbol{x}}(t) = \boldsymbol{F}(\boldsymbol{x}_t)$ is said to be $\Gamma$-equivariant if $\boldsymbol{F}(\gamma\boldsymbol{x}_t) = \gamma\boldsymbol{F}(\boldsymbol{x}_t)$ for all $\gamma \in \Gamma$.

**Lemma 2.1.** *The nonlinear system (16) and the linear system (18) are $\boldsymbol{D}_n$ equivariant.*

**Proof.** We begin with (16), i.e. we let $\boldsymbol{F}$ be as in (17) and $\phi \in \mathcal{C}$. We need only check the equivariance condition on the generators, $\rho, \kappa$, of $\boldsymbol{D}_n$.

$$\begin{aligned} F_i(\rho\phi) &= -(\rho\phi)_i(0) + \alpha f((\rho\phi)_i(-\tau_s)) + \beta[g((\rho\phi)_{i-1}(-\tau)) + g((\rho\phi)_{i+1}(-\tau))] \\ &= -\phi_{i+1}(0) + \alpha f(\phi_{i+1}(-\tau_s)) + \beta[g(\phi_i(-\tau)) + g(\phi_{i+2}(-\tau))] \\ &= F_{i+1}(\phi) \\ &= \rho F_i(\phi) \end{aligned}$$

and

$$\begin{aligned} F_i(\kappa\phi) &= -(\kappa\phi)_i(0) + \alpha f((\kappa\phi)_i(-\tau_s)) + \beta[g((\kappa\phi)_{i-1}(-\tau)) + g((\kappa\phi)_{i+1}(-\tau))] \\ &= -\phi_{n+2-i}(0) + \alpha f(\phi_{n+2-i}(-\tau_s)) + \beta[g(\phi_{n+3-i}(-\tau)) + g(\phi_{n+1-i}(-\tau))] \\ &= F_{n+2-i}(\phi) \\ &= \kappa F_i(\phi). \end{aligned}$$

Thus (16) is $\boldsymbol{D}_n$ equivariant.

For (18), we begin by noting that $L$ may be written component-wise as follows:

$$L_i(\beta)\phi = -\phi_i(0) + \alpha\phi_i(-\tau_s) + \beta[\phi_{i-1}(-\tau) + \phi_{i+1}(-\tau)], \qquad i \,(\mathrm{mod}\ n).$$

The rest of the proof is similar to that for (16). □

## 3. Equivariant Hopf bifurcation

With the structure described above we are now able to state and prove some lemmas which will ultimately lead to our Hopf bifurcation theorem.

To begin with we define

$$v_j = (1, \chi^j, \chi^{2j}, \ldots, \chi^{(n-1)j})^{\mathrm{T}}, \qquad (j = 0, 1, \ldots, n-1), \quad \chi = \mathrm{e}^{(2\pi/n)\mathrm{i}} \tag{21}$$

and note the following properties of the $v_j$:

$$\begin{aligned} &M v_j = (\chi^j + \chi^{-j}) v_j = 2\cos\frac{2\pi j}{n} v_j, \\ &v_i \cdot v_j = \begin{cases} n & i = j, \\ 0 & i \neq j, \end{cases} \\ &\bar{v}_j = v_{n-j}, \qquad (j = 0, 1, \ldots, n-1). \end{aligned} \tag{22}$$

We can now state our first lemma.

**Lemma 3.1.** *Eigenvalue conditions. Let $\alpha, \tau_s, \tau$ be fixed and such that there is a solution, $(\omega_c, \beta_{cj}(\omega_c))$ of (13), for some $j \in \{1, 2, \ldots, [(n-1)/2]\}$, $j \neq n/4$. Then*

- *The characteristic matrix, $\mathcal{M}_n(\lambda)$, is continuously differentiable with respect to $\beta$.*
- *The infinitesimal generator, $A(\beta)$, of the linear operator (19) has a repeated pair of eigenvalues, $\pm\mathrm{i}\omega_c$, at $\beta = \beta_{cj}$.*
- *The generalized eigenspace, $P$, of $A(\beta_{cj})$ for $\pm\mathrm{i}\omega_c$ is spanned by the eigenvectors $\{\mathrm{e}^{\mathrm{i}\omega_c\theta} v_j, \mathrm{e}^{\mathrm{i}\omega_c\theta}\bar{v}_j, \mathrm{e}^{-\mathrm{i}\omega_c\theta}\bar{v}_j, \mathrm{e}^{-\mathrm{i}\omega_c\theta} v_j\}$.*

**Proof.** The differentiability of $\mathcal{M}_n(\lambda)$ follows from its definition (10).

It is clear from the discussion of the previous section that, under the conditions of the lemma, $\Delta_j(\pm\mathrm{i}\omega_c) = 0$ and hence the characteristic equation (11) has a repeated pair of roots $\pm\mathrm{i}\omega_c$. This implies from [17] that $A(\beta_c)$ has a repeated pair of eigenvalues $\pm\mathrm{i}\omega_c$.

Using the properties (22) of the $v_j$, we have

$$\begin{aligned} \mathcal{M}_n(\lambda) v_j &= (\lambda + I - \alpha\mathrm{e}^{-\lambda\tau_s} I) v_j - \beta\mathrm{e}^{-\lambda\tau} M v_j \\ &= \left(\lambda + 1 - \alpha\mathrm{e}^{-\lambda\tau_s} - 2\cos\frac{2\pi j}{n}\beta\mathrm{e}^{-\lambda\tau}\right) v_j \\ &= \Delta_j(\lambda) v_j \end{aligned}$$

and

$$\begin{aligned}\mathcal{M}_n(\lambda)v_{n-j} &= (\lambda + I - \alpha e^{-\lambda\tau_s} I)v_{n-j} - \beta e^{-\lambda\tau} M v_{n-j} \\ &= \left(\lambda + 1 - \alpha e^{-\lambda\tau_s} - 2\cos\frac{2\pi(n-j)}{n}\beta e^{-\lambda\tau}\right) v_{n-j} \\ &= \left(\lambda + 1 - \alpha e^{-\lambda\tau_s} - 2\cos\frac{2\pi j}{n}\beta e^{-\lambda\tau}\right) v_{n-j} \\ &= \Delta_j(\lambda)v_{n-j}.\end{aligned}$$

Thus, under the conditions of the lemma,

$$\mathcal{M}_n(i\omega_c)v_j = \mathcal{M}_n(i\omega_c)v_{n-j} = \mathcal{M}_n(-i\omega_c)\bar{v}_j = \mathcal{M}_n(-i\omega_c)\bar{v}_{n-j} = 0.$$

Noting that $v_{n-j} = \bar{v}_j$ and using a standard result from [17] it follows that $\{e^{i\omega_c\theta}v_j, e^{i\omega_c\theta}\bar{v}_j, e^{-i\omega_c\theta}\bar{v}_j, e^{-i\omega_c\theta}v_j\}$ are eigenvectors of $A(\beta_{cj})$ corresponding to $\pm i\omega_c$. Since there are four linearly independent eigenvectors for the four eigenvalues, the generalized eigenspace $P$ is spanned by these eigenvectors. □

**Lemma 3.2.** *Nonresonance condition. Let $\alpha, \tau_s, \tau$ be fixed and such that there is a solution, $(\omega_c, \beta_{cj}(\omega_c))$ of (13), for some $j \in \{1, 2, \ldots, [(n-1)/2]\}$, $j \neq n/4$. If $\alpha, \tau_s, \tau, \beta_{cj}$ are such that for each $m = 2, 3, \ldots$, and each $k = 0, 1, \ldots, [(n-1)/2]$ at least one of the following is satisfied.*

$$\begin{aligned}1 - \alpha\cos(m\omega_c\tau_s) &\neq 2\beta_{cj}\cos\left(\frac{2\pi k}{n}\right)\cos(m\omega_c\tau), \\ m\omega_c + \alpha\sin(m\omega_c\tau_s) &\neq -2\beta_{cj}\cos\left(\frac{2\pi k}{n}\right)\sin(m\omega_c\tau),\end{aligned} \tag{23}$$

*then all other eigenvalues of $A(\beta_{cj})$ are not integer multiples of $\pm i\omega_c$.*

**Proof.** It is clear from (11)–(13) that for $\beta = \beta_{cj}$, $\Delta_k(\pm i\omega_c) \neq 0$ for $k \neq j$. Thus one-to-one resonances are not possible. Other resonances are possible and occur when there is an integer $m > 1$ such that equations (13) are satisfied for $\omega = \omega_c$ and $\omega = m\omega_c$ with possibly different values of $j$ but with the same values of the parameters, $\alpha, \tau_s, \beta, \tau$. Equations (23) preclude this from happening. □

**Lemma 3.3.** *Transversality condition. Let $\alpha, \tau_s, \tau$ be fixed and such that there is a solution, $(\omega_c, \beta_{cj}(\omega_c))$ of (13), for some $j \in \{1, 2, \ldots, [(n-1)/2]\}$, $j \neq n/4$. If*

$$\cos(\omega_c\tau) + 2\tau\beta_{cj}\cos\left(\frac{2\pi j}{n}\right)\alpha\tau_s\cos(\omega_c(\tau - \tau_s)) \neq 0, \tag{24}$$

*then* $\mathrm{Re}(d\lambda/d\beta)|_{\lambda=i\omega_c} \neq 0$.

**Proof.** Define the characteristic quasi-polynomial via $S(\lambda, \beta) = \prod_{k=0}^{n-1}\Delta_k(\lambda)$ where $\Delta_k(\lambda)$ is as in (12). Since $dS/d\beta = (\partial S/\partial\beta) + (\partial S/\partial\lambda)(d\lambda/d\beta) = 0$, we have

$$\frac{d\lambda}{d\beta} = -\frac{\partial S/\partial\beta}{\partial S/\partial\lambda}. \tag{25}$$

Now for $n$ odd,

$$\frac{\partial S}{\partial\lambda} = \frac{\partial\Delta_0}{\partial\lambda}\prod_{k=1}^{(n-1)/2}\Delta_k^2 + 2\sum_{k=1}^{(n-1)/2}\Delta_0\Delta_k\frac{\partial\Delta_k}{\partial\lambda}\prod_{\substack{i=1\\ i\neq k}}^{(n-1)/2}\Delta_i^2$$

and

$$\frac{\partial S}{\partial \beta} = \frac{\partial \Delta_0}{\partial \beta} \prod_{k=1}^{(n-1)/2} \Delta_k^2 + 2 \sum_{k=1}^{(n-1)/2} \Delta_0 \Delta_k \frac{\partial \Delta_k}{\partial \beta} \prod_{\substack{i=1 \\ i \neq k}}^{(n-1)/2} \Delta_i^2.$$

Putting these in (25), cancelling the common factor $\Delta_j$ from the numerator and denominator, and using $\Delta_j(\mathrm{i}\omega) = 0$, then yields

$$\begin{aligned} \left.\frac{\mathrm{d}\lambda}{\mathrm{d}\beta}\right|_{\lambda=\mathrm{i}\omega} &= -\frac{\partial \Delta_j(\mathrm{i}\omega_c)/\partial\beta}{\partial \Delta_j(\mathrm{i}\omega_c)/\partial\lambda}, \\ &= \frac{2\cos(2\pi j/n)\mathrm{e}^{-\mathrm{i}\omega_c\tau}}{1 + \alpha\tau_s \mathrm{e}^{-\mathrm{i}\omega_c\tau_s} + 2\tau\beta\mathrm{e}^{-\mathrm{i}\omega_c\tau}\cos(2\pi j/n)}. \end{aligned}$$

Repeating the procedure with $n$ even yields the same equation. It follows that

$$\mathrm{Re}\left(\left.\frac{\mathrm{d}\lambda}{\mathrm{d}\beta}\right|_{\lambda=\mathrm{i}\omega_c}\right) = \frac{2\cos(2\pi j/n)(K_1\cos(\omega_c\tau) + K_2\sin(\omega_c\tau))}{K_1^2 + K_2^2},$$

where

$$\begin{aligned} K_1 &= 1 + \alpha\tau_s\cos(\omega_c\tau_s) + 2\tau\beta\cos\left(\frac{2\pi j}{n}\right)\cos(\omega_c\tau), \\ K_2 &= \alpha\tau_s\sin(\omega_c\tau_s) + 2\tau\beta\cos\left(\frac{2\pi j}{n}\right)\sin(\omega_c\tau). \end{aligned} \tag{26}$$

It is then clear that the transversality condition is

$$\cos\left(\frac{2\pi j}{n}\right)(K_1\cos(\omega_c\tau) + K_2\sin(\omega_c\tau)) \neq 0.$$

Note that this implies that $K_1$, $K_2$ are not both zero simultaneously. Using the definitions (26) of $K_1$ and $K_2$ this simplifies to (24). □

From lemmas 2.1, 3.1, 3.2 and 3.3, conditions (H1), (H2) and (H4) of the equivariant Hopf bifurcation theorem [29, theorem 2.1] are satisfied. Further, since the symmetry group and eigenvectors for our model are the same as for the model with $\tau_s = \tau$ it follows from [16, lemma 4] that all other conditions of this theorem are also satisfied. This gives the following theorem.

**Theorem 3.4.** *Let $\alpha$, $\tau_s$, $\tau$ be fixed and such that there is a solution, $(\omega_c, \beta_{cj}(\omega_c))$ of (13), for some $j \in \{1, 2, \ldots, [(n-1)/2]\}$, $j \neq n/4$. If conditions (23), (24) hold then system (1) undergoes an equivariant Hopf bifurcation as $\beta$ varies through $\beta_{cj}$.*

## 4. Centre manifold reduction

From the discussion of the previous subsection, we know that the characteristic equation (11) has a repeated pair of purely imaginary eigenvalues $\pm\mathrm{i}\omega$ under condition (13). In this section we will obtain explicit analytical expressions for the stability condition of equivariant Hopf bifurcation solutions by reducing system (1) to its centre manifold. To do this we first express the delay equation as an abstract evolution equation on the phase space $\mathcal{C}$, namely,

$$\dot{\boldsymbol{x}}_t = A(\beta)\boldsymbol{x}_t + \boldsymbol{G}(\boldsymbol{x}_t), \tag{27}$$

where $A(\beta)$ is defined in (20) and the nonlinear operator $\boldsymbol{G} : \mathcal{C} \to \mathcal{C}$ is in the form of

$$\boldsymbol{G}(\phi)(\theta) = \begin{cases} 0 & \text{for } \theta \in [-h,\ 0), \\ \hat{\boldsymbol{F}}(\phi) & \text{for } \theta = 0, \end{cases} \tag{28}$$

with $\hat{\boldsymbol{F}}(\phi) = \boldsymbol{F}(\phi) - (A(\beta)\phi)(0)$ and $\boldsymbol{F}$ is defined by (17).

We must also restrict our parameter values more than in theorem 3.4. In particular we need to ensure that $A(\beta_{cj})$ has no other eigenvalues with zero real part. This can be done by assuming that $\alpha, \tau_s, \tau$ are such that when $\beta = \beta_{cj}$ there is no $\omega \neq \omega_c$ such that (13) are satisfied, for any $j \in \{0, 1, 2, \ldots, [(n-1)/2]\}$. We note that this eliminates a set of parameter values of measure zero from the four-dimensional parameter space. Under these conditions, $\mathcal{C}$ can be split into two subspaces as $\mathcal{C} = P \oplus Q$, where $P$ is as defined in lemma 3.1, while $Q$ is the complementary space of $P$.

It follows from lemma 3.1 that we can choose the basis of $P$ as

$$\begin{aligned}\Phi(\theta) &= (\phi_1(\theta), \phi_2(\theta), \phi_3(\theta), \phi_4(\theta)) \\ &= (\mathrm{e}^{\mathrm{i}\omega_c\theta} v_j, \mathrm{e}^{-\mathrm{i}\omega_c\theta} \bar{v}_j, \mathrm{e}^{\mathrm{i}\omega_c\theta} \bar{v}_j, \mathrm{e}^{-\mathrm{i}\omega_c\theta} v_j),\end{aligned} \tag{29}$$

where $v_j$ is given in (21).

Then for $u \in \mathcal{C}$ and $v \in \mathcal{C}^*$, we can define a bilinear operator:

$$\langle v, u\rangle = \bar{v}^{\mathrm{T}}(0)u(0) - \int_{-h}^{0}\int_{0}^{\theta} \bar{v}^{\mathrm{T}}(\xi - \theta)[\mathrm{d}\eta(\theta)]u(\xi)\,\mathrm{d}\xi, \tag{30}$$

where the matrix $\eta(\theta)$ is given by

$$\begin{aligned}\eta(\theta) &= \begin{pmatrix} -\delta_0 + \alpha\delta_{\tau_s} & \beta\delta_\tau & 0 & \cdots & 0 & \beta\delta_\tau \\ \beta\delta_\tau & -\delta_0 + \alpha\delta_{\tau_s} & \beta\delta_\tau & 0 & \cdots & 0 \\ & & & \vdots & & \\ \beta\delta_\tau & 0 & \cdots & 0 & \beta\delta_\tau & -\delta_0 + \alpha\delta_{\tau_s} \end{pmatrix} \\ &= (-\delta_0 + \alpha\delta_{\tau_s})I + \beta\delta_\tau M\end{aligned} \tag{31}$$

and $\delta_u = \delta(\theta + u)$ is the Dirac distribution at the point $\theta = -u$.

Now $\bar{\Phi}^{\mathrm{T}}(\xi - \theta)\eta(\theta)\Phi(\xi)$ can be simplified to

$$\bar{\Phi}^{\mathrm{T}}(\xi - \theta)\eta(\theta)\Phi(\xi) = \left[-\delta(\theta) + \alpha\delta(\theta + \tau_s) + 2\beta\cos\frac{2\pi j}{n}\delta(\theta + \tau)\right]\bar{\Phi}^{\mathrm{T}}(\xi - \theta)\Phi(\xi).$$

Thus from $K = \langle \bar{\Phi}^{\mathrm{T}}, \Phi\rangle$, we can construct the basis for the subspace in $\mathcal{C}^*$ corresponding to $P$:

$$\begin{aligned}\Psi(\xi) &= K^{-1}\bar{\Phi}^{\mathrm{T}}(\xi) \\ &= \frac{1}{n}\begin{pmatrix} \bar{a}^{-1}\mathrm{e}^{-\mathrm{i}\omega\xi}\bar{v}_j^{\mathrm{T}} \\ a^{-1}\mathrm{e}^{\mathrm{i}\omega\xi} v_j^{\mathrm{T}} \\ \bar{a}^{-1}\mathrm{e}^{-\mathrm{i}\omega\xi} v_j^{\mathrm{T}} \\ a^{-1}\mathrm{e}^{\mathrm{i}\omega\xi}\bar{v}_j^{\mathrm{T}} \end{pmatrix}\end{aligned} \tag{32}$$

where $a = 1 - \alpha(\tau - \tau_s)(\cos(\omega\tau_s) + \mathrm{i}\sin(\omega\tau_s)) + (1 - \mathrm{i}\omega)\tau$.

Therefore,

$$\Psi(0) = \frac{1}{n}\begin{pmatrix} \bar{a}^{-1}\bar{v}_j^{\mathrm{T}} \\ a^{-1} v_j^{\mathrm{T}} \\ \bar{a}^{-1} v_j^{\mathrm{T}} \\ a^{-1}\bar{v}_j^{\mathrm{T}} \end{pmatrix}. \tag{33}$$

Define $\boldsymbol{z} \equiv (z_1, z_2, z_3, z_4)^{\mathrm{T}}$ where $z_2 = \bar{z}_1$, $z_4 = \bar{z}_3$ is the local coordinate system on the four-dimensional centre manifold induced by the basis $\Phi$. With the aid of equations (29) and (32), one can decompose $\boldsymbol{x}_t$ into two parts:

$$\boldsymbol{x}_t = \boldsymbol{x}_t^P + \boldsymbol{x}_t^Q = \Phi\langle\Psi, \boldsymbol{x}_t\rangle + \boldsymbol{x}_t^Q = \Phi\boldsymbol{z} + \boldsymbol{x}_t^Q, \tag{34}$$

which implies that the projection of $\boldsymbol{x}_t$ on the centre manifold is $\Phi z$. Using the decomposition (34) in (27) results in

$$\langle \Psi, \Phi \rangle \dot{z} = \langle \Psi, A(\beta_{cj})\Phi \rangle z + \langle \Psi, \boldsymbol{G}(t, \Phi z + x_t^Q) \rangle$$

then, to lowest order, the dynamical system describing the flow on the centre manifold can be written as

$$\dot{z}(t) = Bz(t) + \Psi(0)\hat{\boldsymbol{F}}(\Phi(\theta)z(t)), \tag{35}$$

where

$$B = \begin{pmatrix} \mathrm{i}\omega_c & 0 & 0 & 0 \\ 0 & -\mathrm{i}\omega_c & 0 & 0 \\ 0 & 0 & \mathrm{i}\omega_c & 0 \\ 0 & 0 & 0 & -\mathrm{i}\omega_c \end{pmatrix}. \tag{36}$$

Under the conditions (2) and (3) the nonlinear part of the system is

$$\hat{F}_i(\boldsymbol{x}_t) = \frac{1}{3!}[\alpha\delta_1 x_{t,i}^3(-\tau_s) + \beta_{cj}\delta_2 x_{t,i-1}^3(-\tau) + \beta_{cj}\delta_2 x_{t,i+1}^3(-\tau)] + O(\|\boldsymbol{x}\|^4)$$

for $i \pmod n$, where $\delta_1 = f'''(0)$ and $\delta_2 = g'''(0)$. Further,

$$\begin{aligned} \Phi(\theta)z(t) &= (\mathrm{e}^{\mathrm{i}\omega_c\theta} z_1 + \mathrm{e}^{-\mathrm{i}\omega_c\theta} z_4)v_j + (\mathrm{e}^{-\mathrm{i}\omega_c\theta} z_2 + \mathrm{e}^{\mathrm{i}\omega_c\theta} z_3)\bar{v}_j \\ &= A_1 v_j + A_2 \bar{v}_j, \end{aligned} \tag{37}$$

so the $k$th component in $(\Phi(\theta)z(t))^3$ is

$$\begin{aligned} (\Phi(\theta)z(t))_k^3 &= (A_1 v_j + A_2 \bar{v}_j)_k^3 \\ &= (A_1 \chi^{(k-1)j} + A_2 \bar{\chi}^{(k-1)j})^3 \\ &= A_1^3 \chi^{3(k-1)j} + A_2^3 \bar{\chi}^{3(k-1)j} + 3A_1^2 A_2 \chi^{(k-1)j} + 3A_1 A_2^2 \bar{\chi}^{(k-1)j} \end{aligned} \tag{38}$$

and

$$\hat{F}_i(\Phi(\theta)z(t)) = \frac{1}{3!}[\alpha\delta_1(\Phi(-\tau_s)z)_i^3 + \beta\delta_2(\Phi(-\tau)z)_{i-1}^3 + \beta\delta_2(\Phi(-\tau)z)_{i+1}^3] + O(\|z\|^4),$$

for $i \pmod n$.

In vector form, this can be written as

$$\begin{aligned} \hat{\boldsymbol{F}}(\Phi(\theta)z(t)) = \frac{1}{3!}\{&\alpha\delta_1[A_1^3(-\tau_s)v_j^3 + 3A_1^2(-\tau_s)A_2(-\tau_s)v_j^2\bar{v}_j + 3A_1(-\tau_s)A_2^2(-\tau_s)v_j\bar{v}_j^2 \\ &+A_2^3(-\tau_s)\bar{v}_j^3] + \beta\delta_2[A_1^3(-\tau)Mv_j^3 + 3A_1^2(-\tau)A_2(-\tau)Mv_j^2\bar{v}_j \\ &+3A_1(-\tau)A_2^2(-\tau)Mv_j\bar{v}_j^2 + A_2^3(-\tau)M\bar{v}_j^3]\}. \end{aligned}$$

Thus it follows that

$$\Psi(0)\hat{\boldsymbol{F}}(\Phi z) = \frac{1}{2}\begin{pmatrix} \bar{a}^{-1}\left(\alpha\delta_1\mathcal{A}_1^2\mathcal{A}_2 + 2\beta\delta_2\cos\dfrac{2\pi j}{n}\mathcal{B}_1^2\mathcal{B}_2\right) \\ a^{-1}\left(\alpha\delta_1\mathcal{A}_1\mathcal{A}_2^2 + 2\beta\delta_2\cos\dfrac{2\pi j}{n}\mathcal{B}_1\mathcal{B}_2^2\right) \\ \bar{a}^{-1}\left(\alpha\delta_1\mathcal{A}_1\mathcal{A}_2^2 + 2\beta\delta_2\cos\dfrac{2\pi j}{n}\mathcal{B}_1\mathcal{B}_2^2\right) \\ a^{-1}\left(\alpha\delta_1\mathcal{A}_1^2\mathcal{A}_2 + 2\beta\delta_2\cos\dfrac{2\pi j}{n}\mathcal{B}_1^2\mathcal{B}_2\right) \end{pmatrix}, \tag{39}$$

where $\mathcal{A}_k, \mathcal{B}_k$ $(k = 1, 2)$ come from $A_k$ when $\theta$ is $-\tau_s$ or $-\tau$, respectively. That is

$$\begin{aligned} \mathcal{A}_1 &= \mathrm{e}^{-\mathrm{i}\omega_c\tau_s} z_1 + \mathrm{e}^{\mathrm{i}\omega_c\tau_s} z_4, \qquad & \mathcal{A}_2 &= \mathrm{e}^{\mathrm{i}\omega_c\tau_s} z_2 + \mathrm{e}^{-\mathrm{i}\omega_c\tau_s} z_3, \\ \mathcal{B}_1 &= \mathrm{e}^{-\mathrm{i}\omega_c\tau} z_1 + \mathrm{e}^{\mathrm{i}\omega_c\tau} z_4, \qquad & \mathcal{B}_2 &= \mathrm{e}^{\mathrm{i}\omega_c\tau} z_2 + \mathrm{e}^{-\mathrm{i}\omega_c\tau} z_3. \end{aligned} \tag{40}$$

Therefore, the dynamical system on the centre manifold is

$$\begin{pmatrix} \dot{z}_1 \\ \dot{z}_2 \\ \dot{z}_3 \\ \dot{z}_4 \end{pmatrix} = \begin{pmatrix} \mathrm{i}\omega & 0 & 0 & 0 \\ 0 & -\mathrm{i}\omega & 0 & 0 \\ 0 & 0 & \mathrm{i}\omega & 0 \\ 0 & 0 & 0 & -\mathrm{i}\omega \end{pmatrix} \begin{pmatrix} z_1 \\ z_2 \\ z_3 \\ z_4 \end{pmatrix} + \frac{1}{2} \begin{pmatrix} \bar{a}^{-1} \left( \alpha\delta_1 \mathcal{A}_1^2 \mathcal{A}_2 + 2\beta\delta_2 \cos\dfrac{2\pi j}{n} \mathcal{B}_1^2 \mathcal{B}_2 \right) \\ a^{-1} \left( \alpha\delta_1 \mathcal{A}_1 \mathcal{A}_2^2 + 2\beta\delta_2 \cos\dfrac{2\pi j}{n} \mathcal{B}_1 \mathcal{B}_2^2 \right) \\ \bar{a}^{-1} \left( \alpha\delta_1 \mathcal{A}_1 \mathcal{A}_2^2 + 2\beta\delta_2 \cos\dfrac{2\pi j}{n} \mathcal{B}_1 \mathcal{B}_2^2 \right) \\ a^{-1} \left( \alpha\delta_1 \mathcal{A}_1^2 \mathcal{A}_2 + 2\beta\delta_2 \cos\dfrac{2\pi j}{n} \mathcal{B}_1^2 \mathcal{B}_2 \right) \end{pmatrix} + O(\|z\|^4). \tag{41}$$

After normal form transformation of the cubic terms, the coefficients of the resonant monomial (in this case, it includes the terms $y_1^i\, y_2^j\, y_3^k\, y_4^l$ where $i, j, k, l$ satisfy

$$\begin{cases} i + j + k + l = 3, \\ i - j + k - l = \pm 1, \end{cases}$$

'+' in equations $\dot{y}_1, \dot{y}_3$, '−' in equations $\dot{y}_2, \dot{y}_4$) are unchanged [4]. Therefore the normal form truncated to degree three is:

$$\begin{aligned} \dot{y}_1 &= \mathrm{i}\omega y_1 + \bar{a}^{-1}\bar{b}(y_1 y_2 + 2y_3 y_4) y_1, \\ \dot{y}_2 &= -\mathrm{i}\omega y_2 + a^{-1} b(y_1 y_2 + 2y_3 y_4) y_2, \\ \dot{y}_3 &= \mathrm{i}\omega y_3 + \bar{a}^{-1}\bar{b}(y_3 y_4 + 2y_1 y_2) y_3, \\ \dot{y}_4 &= -\mathrm{i}\omega y_4 + a^{-1} b(y_3 y_4 + 2y_1 y_2) y_4, \end{aligned} \tag{42}$$

where $b = \frac{1}{2}[\delta_2(1 - \mathrm{i}\omega) + (\delta_1 - \delta_2)\alpha\mathrm{e}^{\mathrm{i}\omega\tau_s}]$.

Noting that $y_1 = \bar{y}_2$ and $y_3 = \bar{y}_4$ and using the transformation

$$\begin{aligned} \xi_1(t) &= y_2(s), \\ \xi_2(t) &= y_4(s), \end{aligned} \tag{43}$$

with $s = ((1 + p)\omega)^{-1} t$, where $p$ is the period of the bifurcating solutions, the normal form up to the third order can be written as

$$\begin{aligned} (1 + p)\dot{\xi}_1 &= -\mathrm{i}\xi_1(t) + a^{-1} b\omega^{-1}(|\xi_1(t)|^2 + 2|\xi_2(t)|^2)\xi_1(t), \\ (1 + p)\dot{\xi}_2 &= -\mathrm{i}\xi_2(t) + a^{-1} b\omega^{-1}(2|\xi_1(t)|^2 + |\xi_2(t)|^2)\xi_2(t). \end{aligned} \tag{44}$$

In vector form this becomes

$$(1 + p)\dot{\boldsymbol{\xi}} + h(\boldsymbol{\xi}) = 0,$$

where $\boldsymbol{\xi} = (\xi_1, \xi_2) \in C \oplus C$ and

$$h(\boldsymbol{\xi}) = \begin{pmatrix} \mathrm{i}\xi_1 - a^{-1} b\omega^{-1}(|\xi_1(t)|^2 + 2|\xi_2(t)|^2)\xi_1 \\ \mathrm{i}\xi_2 - a^{-1} b\omega^{-1}(2|\xi_1(t)|^2 + |\xi_2(t)|^2)\xi_2 \end{pmatrix}.$$

From [29], we know that the bifurcations of small-amplitude periodic solutions are determined by the zeros of the equation

$$h(\boldsymbol{\xi}) - \mathrm{i}(1+p)\boldsymbol{\xi} = 0 \tag{45}$$

and that their (orbital) stability is determined by the sign of eigenvalues of

$$Dh(\boldsymbol{\xi}) - \mathrm{i}(1+p)I = 0.$$

More precisely, we rewrite (45) as

$$A\begin{pmatrix}\xi_1\\ \xi_2\end{pmatrix} + B\begin{pmatrix}\xi_1^2\bar{\xi}_1\\ \xi_2^2\bar{\xi}_2\end{pmatrix} = 0$$

with

$$A = A_0 + A_N(|\xi_1(t)|^2 + |\xi_2(t)|^2), \qquad B = B_0,$$

where $A_0 = -\mathrm{i}p$, $A_N = -2a^{-1}b\omega^{-1}$, $B_0 = a^{-1}b\omega^{-1}$. Now,

$$\begin{aligned}\mathrm{Re}(B_0) &= \mathrm{Re}(a^{-1}b\omega^{-1})\\ &= \omega^{-1}\mathrm{Re}(a^{-1}b)\\ &= \frac{\omega^{-1}}{2}\frac{m}{[1+\tau-\alpha(\tau-\tau_s)\cos(\omega\tau_s)]^2+[\omega\tau+\alpha(\tau-\tau_s)\sin(\omega\tau_s)]^2} \equiv \mathcal{W},\end{aligned} \tag{46}$$

where

$$\begin{aligned}m &= \delta_2[1+\tau(1+\omega^2)-\alpha(\tau-\tau_s)(\cos(\omega\tau_s)-\omega\sin(\omega\tau_s))]\\ &\quad+(\delta_1-\delta_2)\alpha[(1+\tau)\cos(\omega\tau_s)-\alpha(\tau-\tau_s)-\omega\tau\sin(\omega\tau_s)].\end{aligned} \tag{47}$$

But $A_N = -2B_0$, so

$$\mathrm{Re}(A_N + B_0) = \mathrm{Re}(-B_0) = -\mathcal{W}, \tag{48}$$

$$\mathrm{Re}(2A_N + B_0) = \mathrm{Re}(-3B_0) = -3\mathcal{W}. \tag{49}$$

From the results of [12] the criticality and stability of the bifurcating solutions depend on the signs of $\mathrm{Re}(B_0)$, $\mathrm{Re}(A_N + B_0)$ and $\mathrm{Re}(2A_N + B_0)$. Clearly, for our model there are only two cases to consider:

(i) if $m < 0$, then $\mathrm{Re}(B_0) < 0$, $\mathrm{Re}(A_N + B_0) > 0$ and $\mathrm{Re}(2A_N + B_0) > 0$;
(ii) if $m > 0$, then $\mathrm{Re}(B_0) > 0$, $\mathrm{Re}(A_N + B_0) < 0$ and $\mathrm{Re}(2A_N + B_0) < 0$.

Combining the discussion above and the results given in [16] and [30] we have the following theorem.

**Theorem 4.1.** *Suppose that for some $j \in \{1, 2, \ldots, [(n-1)/2], j \neq n/4\}$ conditions (13) are satisfied, i.e. the parameters are such that the characteristic equation has a repeated pair of imaginary roots $\pm\mathrm{i}\omega$ given by $\Delta_j(\pm\mathrm{i}\omega) = 0$. Then there exists $2(n+1)$ branches of asynchronous periodic solutions of period $p$ near $2\pi/\omega$ bifurcated from the zero solution of the system. In particular, there are*

*(1) 2 phase-locked oscillations: $x_i(t) = x_{i+1}(t \pm (jp/n))$ for $i \pmod n$; when $m < 0$, they are supercritical and have the stability the trivial solution had before the bifurcation; when $m > 0$, they are subcritical and orbitally unstable;*
*(2) $n$ unstable mirror-reflecting waves: $x_i(t) = x_{n+2k-i}(t)$ for $i \pmod n$ and $k = 1, 2, \ldots, n$; when $m < 0$, they are supercritical, whereas when $m > 0$, they are subcritical;*
*(3) $n$ unstable standing waves: $x_i(t) = x_{n+2k-i}(t-(p/2))$ for $i \pmod n$ and $k = 1, 2, \ldots, n$; when $m < 0$, they are supercritical, whereas when $m > 0$, they are subcritical.*

Although the expression for $m$ is complicated, we have the following general result.

**Theorem 4.2.** *Let $\alpha, \tau_s, \delta_j$ be fixed with $\delta = \delta_1/\delta_2$. If $\alpha < 0, \delta_2 < 0$, $\tau_s < (\pi/2)\min(1, 1/(\delta-2))$ and $|\alpha| < \min(1, 1/\tau_s, 1/|\delta-1|, 1/|\delta-2|\tau_s)$, then $m < 0$.*

**Proof.** Rewrite $m$ in the following manner

$$m = \delta_2\{[1+\alpha^2(\delta-1)\tau_s + (\delta-1+\tau_s)\alpha\cos\omega\tau_s] + \tau[1-\alpha^2(\delta-1)+(\delta-2)\alpha\cos\omega\tau_s] + \omega[\tau(\omega-\alpha(\delta-2)\sin\omega\tau_s) - \alpha\tau_s\sin\omega\tau_s]\}.$$

It is easy to show the first two terms are positive as follows.

$$\begin{aligned} 1+\alpha^2(\delta-1)\tau_s + (\delta-1+\tau_s)\alpha\cos\omega\tau_s &\geqslant 1+\alpha^2(\delta-1)\tau_s - |\delta-1+\tau_s||\alpha| \\ &= \begin{cases} ((\delta-1)|\alpha|-1)(\tau_s|\alpha|-1) & \text{if } \delta-1+\tau_s \geqslant 0 \\ ((\delta-1)|\alpha|+1)(\tau_s|\alpha|+1) & \text{if } \delta-1+\tau_s < 0 \end{cases} \\ &> 0 \end{aligned}$$

since $|\alpha| < \min(1/\tau_s, 1/|\delta-1|)$.

$$\begin{aligned} \tau[1-\alpha^2(\delta-1)+(\delta-2)\alpha\cos\omega\tau_s] &\geqslant \tau[1-\alpha^2(\delta-1)-|\delta-2||\alpha|] \\ &= \begin{cases} -\tau((\delta-1)|\alpha|-1)(|\alpha|+1) & \text{if } \delta-2 \geqslant 0 \\ -\tau((\delta-1)|\alpha|+1)(|\alpha|-1) & \text{if } \delta-2 < 0 \end{cases} \\ &> 0 \end{aligned}$$

since $|\alpha| < \min(1, 1/|\delta-1|)$.

Now consider the third term, $\omega[\tau(\omega-\alpha(\delta-2)\sin\omega\tau_s) - \alpha\tau_s\sin\omega\tau_s]$. Since $|\alpha| < 1/|\delta-2|\tau_s$,

$$\omega - \alpha(\delta-2)\sin\omega\tau_s \geqslant \omega(1-|\alpha||\delta-2|\tau_s) > 0.$$

Recalling that $\alpha < 0$ and $\tau_s \geqslant 0$, it follows that the third term is positive if $\sin\omega\tau_s \geqslant 0$. Rewriting the third term as $\omega[\omega\tau - ((\delta-2)\tau+\tau_s)\alpha\sin\omega\tau_s]$, it is clear that the third term is also positive if $\sin\omega\tau_s < 0$ and $(\delta-2)\tau+\tau_s \leqslant 0$.

It remains to consider the third term when $\sin\omega\tau_s < 0$ and $\tau(\delta-2)+\tau_s > 0$. Note that this implies $\omega\tau_s \in ((2k+1)\pi, (2k+2)\pi)$, $k = 0, 1, \ldots$. Consider first the case when $\beta\cos(2\pi j/n) < 0$. From (13) it is easy to see that this implies $\cos\omega\tau < 0$ and $\sin\omega\tau > 0$; thus $\omega\tau \in ((2k+\frac{1}{2})\pi, (2k+1)\pi)$, $k = 0, 1, \ldots$. Thus on the $k$th interval we have

$$\begin{aligned} \omega\tau - ((\delta-2)\tau+\tau_s)\alpha\sin\omega\tau_s &\geqslant \begin{cases} \omega\tau-\tau_s & \text{if } \delta-2 \leqslant 0 \\ \omega\tau-[\tau_s+(\delta-2)\tau] & \text{if } \delta-2 > 0 \end{cases} \\ &= \begin{cases} \omega\tau-\tau_s & \text{if } \delta-2 \leqslant 0 \\ \omega\tau-\tau_s\left[1+(\delta-2)\dfrac{\omega\tau}{\omega\tau_s}\right] & \text{if } \delta-2 > 0 \end{cases} \\ &> \begin{cases} \left(2k+\dfrac{1}{2}\right)\pi-\tau_s & \text{if } \delta-2 \leqslant 0 \\ \left(2k+\dfrac{1}{2}\right)\pi-\tau_s\left[1+(\delta-2)\dfrac{(2k+1)\pi}{\omega\tau_s}\right] & \text{if } \delta-2 > 0 \end{cases} \\ &> 0, \end{aligned}$$

since $0 < \alpha\sin\omega\tau < 1$, $\tau_s < (\pi/2)\min(1, 1/(\delta-2))$ and $\omega\tau_s > \pi$. The proof for $\beta\cos(2\pi j/n) > 0$ is similar. □

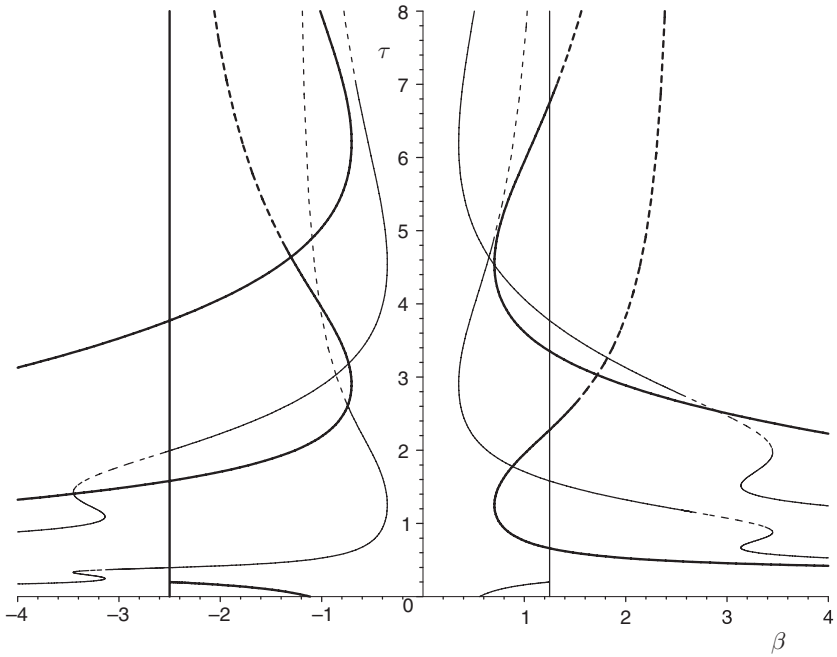


**Figure 2.** Bifurcation set for (1) with $n = 3, \alpha = -1.5, \tau_s = 1, f(u) = \tanh(u)$ and $g(u) = (1/\gamma)\tanh(\gamma u)$ and $\gamma = 0.4$. Thin/thick curves correspond to standard/equivariant Hopf bifurcations; thin/thick vertical lines to standard/equivariant pitchfork bifurcations. Supercritical/subcritical bifurcations (as predicted by the theory) are indicated by solid/dashed lines.

## 5. Comparison with numerical continuation: an example

To supplement our theoretical work, we consider a particular example and compare the predictions of theorem 4.1 with the stability and criticality predicted by the program DDE-BIFTOOL [10]. This program performs numerical continuation of a periodic orbit emanating from a Hopf bifurcation of a delay differential equation and numerical computation of the Floquet multipliers of the periodic orbit. To perform the numerical computations, we must specify the nonlinearities; thus we take $f(u) = \tanh(u)$ and $g(u) = (1/\gamma)\tanh(\gamma u)$. With these functions the critical quantity $m$ becomes

$$m = -2\gamma^2[1 + \tau(1+\omega^2) + \alpha^2(\tau - \tau_s) - \alpha\cos\omega\tau_s - \alpha(2\tau - \tau_s)(\cos\omega\tau_s - \omega\sin\omega\tau_s)] - 2\alpha[(1+\tau)\cos\omega\tau_s - \alpha(\tau - \tau_s) - \omega\tau\sin\omega\tau_s].$$

As shown in [6, 31], for fixed $n, \alpha, \tau_s$ the locus of Hopf bifurcations of the trivial solution of (1) can be represented as curves in the $\beta, \tau$ parameter space. Figure 2 shows what these curves look like for $n = 3, \alpha = -1.5$ and $\tau_s = 1$. Thick lines correspond to equivariant bifurcations and thin lines to standard bifurcations. Note that these curves are identical for all values of $\gamma$. The trivial solution is asymptotically stable in the region contiguous with the $\tau$ axis. To evaluate the sign of $m$ we specify $\gamma$, a point of equivariant Hopf bifurcation (i.e. a point $(\beta, \tau)$ on one of the thick curves) and the corresponding value of $\omega$. The latter two can be done by specifying $\tau$ and solving equations (14) and (15) for $\omega$ and $\beta$. Taking $n = 3, \alpha = -1.5$ and $\tau_s = 1$ and evaluating $m$ at each point of the equivariant Hopf bifurcation curves we find the following. With $\gamma = 1, m < 0$ everywhere on the curves, whereas with $\gamma = 0.4, m$ is positive

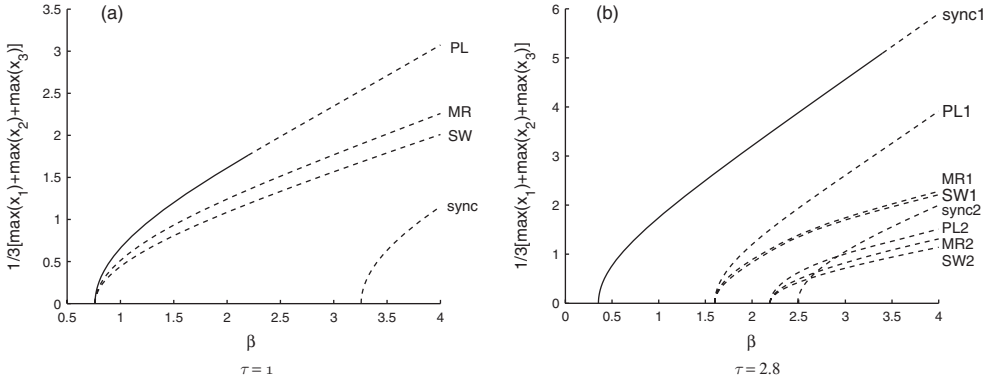


**Figure 3.** Numerical continuation of periodic solutions emanating from Hopf bifurcations of (1) with $n = 3$, $\alpha = -1.5$, $\tau_s = 1$, $f(u) = \tanh(u) = g(u)$, i.e. $\gamma = 1$. Branches from standard Hopf are indicated by 'sync', branches from equivariant Hopf are indicated by 'PL' (phase-locked), 'MR' (mirror reflecting) and 'SW' (standing waves). Solid/dashed lines indicate stable/unstable solutions.

at some points and negative at others. The sign of $m$ for $\gamma = 0.4$ is indicated in figure 2, with solid thick lines corresponding to $m < 0$ and dashed thick lines to $m > 0$.

Recall from theorem 4.1 that $m < 0$ corresponds to the branches of asynchronous periodic orbits being supercritical and $m > 0$ corresponds to the branches being subcritical. The mirror-reflecting and standing waves are predicted to be always unstable at bifurcation. The phase-locked oscillations are predicted to be stable when $m < 0$ and the bifurcation is at parameter values which lie on the boundary of the stability region of the trivial solution; otherwise it is unstable. Thus for $\gamma = 1$ we expect that all branches will be supercritical and those branches which border on the stability region will give rise to stable phase-locked oscillations. For $\gamma = 0.4$ the branches may be super- or subcritical depending on the values of $\beta$, $\gamma$ where the Hopf bifurcation occurs.

The stability and criticality of the standard Hopf bifurcation (which gives rise to synchronous oscillations) was studied in [31]. With the parameters $n = 3, \alpha = -1.5, \tau_s = 1$, it can be shown that for $\gamma = 1$ the standard Hopf is always supercritical. For $\gamma = 0.4$, the standard Hopf is supercritical for some values of $\beta$ and $\tau$ (shown by solid thin lines in figure 2) and subcritical and unstable for others (shown by dashed thin lines in figure 2). At a point $(\beta, \tau)$ where the bifurcation is supercritical the resulting oscillatory solution is stable if the point lies on the boundary of the stability region of the trivial solution, otherwise it is unstable.

We performed numerical continuation studies of (1) using $\beta$ as the continuation (bifurcation) parameter. The other parameters were fixed at $n = 3, \alpha = -1.5, \tau_s = 1, \gamma = 1$ or 0.4 and various values of $\tau$. The results are shown in figures 3 and 4. Each plot shows a measure of the amplitude of the periodic solution versus $\beta$. The measure used is $\frac{1}{3}(\max_{t\in[0,T]} x_1(t) + \max_{t\in[0,T]} x_2(t) + \max_{t\in[0,T]} x_3(t))$, where $T$ is the period of the orbit. Branches of stable/unstable periodic solutions are indicated by solid/dashed lines.

Figure 3 shows the results for $\gamma = 1$ (which corresponds to $f = g = \tanh$) and two values of $\tau$. As predicted by the theory, all branches are supercritical, and the mirror reflecting and standing wave branches are unstable. Figure 3(*a*) corresponds to $\tau = 1$ where the equivariant Hopf bifurcation lies on the boundary of the stability region of the trivial solution (at $\beta \approx 0.75$) and the standard Hopf lies to the right of this (at $\beta \approx 3.25$). As predicted, the branch of phase-locked oscillations is stable at bifurcation, while the branch of synchronous oscillations is unstable. Figure 3(*b*) shows the reverse situation. It also shows a second equivariant bifurcation

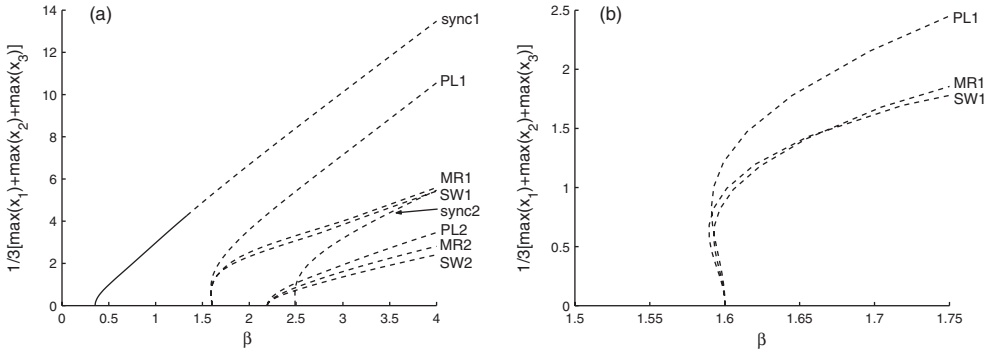


All branches. Closeup of equivariant Hopf showing subcritical behaviour.

**Figure 4.** Numerical continuation of periodic solutions emanating from Hopf bifurcations of (1) with $n = 3$, $\alpha = -1.5$, $\tau_s = 1, \tau = 1$, $f(u) = \tanh(u)$, $g(u) = (1/\gamma)\tanh(\gamma u)$ and $\gamma = 0.4$. Branch labelling is as in figure 3.

and a second standard Hopf which give rise to unstable oscillations since they occur at larger values of $\beta$.

Figure 4 shows the results when $\gamma = 0.4$ and $\tau = 2.8$. The predictions of the theory in this case may be checked by drawing a horizontal line in figure 2 at $\tau = 2.8$. This line crosses four curves as $\beta$ increases from zero, corresponding to four points of Hopf bifurcation. At $\beta \approx 0.3$ there is a supercritical standard Hopf, at $\beta \approx 1.6$ there is subcritical equivariant Hopf, at $\beta \approx 2.2$ there is a second equivariant Hopf which is supercritical and at $\beta \approx 2.5$ there is a second standard Hopf which is subcritical. Since the first standard Hopf bifurcation point is the only one that lies on the stability boundary of the trivial solution, its corresponding branch of periodic solutions is the only one that can be stable. This is exactly what we see in figure 4(*a*). Figure 4(*b*) shows a close-up of the subcritical equivariant Hopf. Note that the branch turns over quite quickly. This is not unexpected, since this value of $\tau$ is close to the point where the bifurcation curve changes from being subcritical to supercritical.

## 6. Discussion

We established conditions under which an equivariant Hopf bifurcation occurs in the ring neural network (1) and showed that for a ring with $n$ elements there are $[(n-1)/2]$ of these bifurcations. Using centre manifold reduction, normal form analysis and equivariant bifurcation theory, we showed that each of these bifurcations gives rise to $2(n+1)$ branches of periodic orbits: 2 phase-locked oscillations, $n$ mirror reflecting waves and $n$ standing waves. We described a quantity, a complicated function of the system parameters, which determines whether the bifurcation is supercritical or subcritical. Finally, we showed that the mirror reflecting waves and standing waves are always unstable, while the phase locked oscillations are stable if (i) the bifurcation is supercritical and (ii) the bifurcation occurs on the boundary of the region of stability of the trivial solution.

Putting this together with our previous work [31], which studied the region of stability of the trivial solution of our model and the criticality of standard Hopf bifurcations, our theoretical results give an accurate picture of the bifurcation structure, in the neighbourhood of the bifurcation point, for any set of parameter values and nonlinearities (satisfying the conditions (2) and (3)). By contrast, numerical continuations such as those of section 5 give

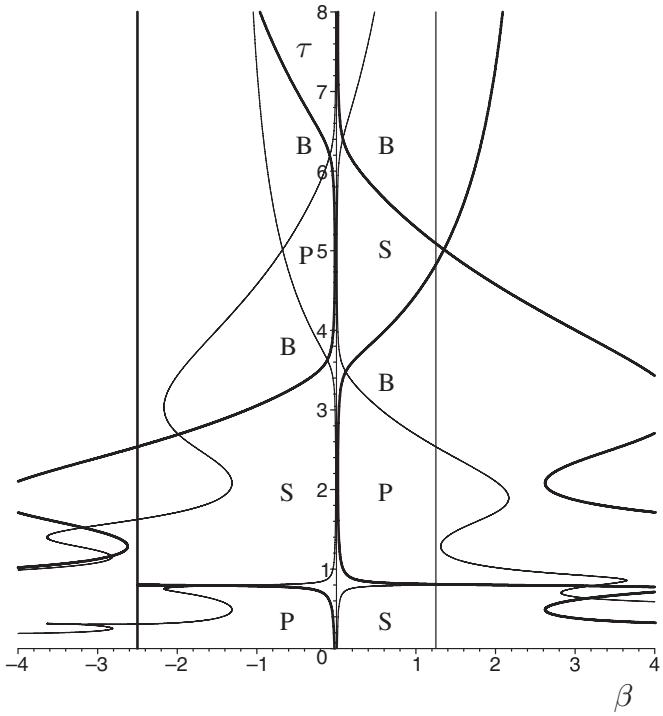


**Figure 5.** Bifurcation set for (1) with $n = 3, \alpha = -1.5, \tau_s = 2$. Thin/thick curves correspond to standard/equivariant Hopf bifurcations; thin/thick vertical lines to standard/equivariant pitchfork bifurcations. All curves are supercritical with $\gamma = 1$. Regions where the synchronized/phase-locked oscillations are stable are indicated by S/P. Stability close to the bifurcation curves is predicted by the theory. Stability further from the curves is verified by numerical simulations. Regions where bistability between the two oscillations is observed in numerical simulations are indicated by B.

us information corresponding to a specific nonlinearity and set of parameter values, but can tell us about the stability of periodic orbits for values of the bifurcation parameter far from the bifurcation point. These results are complementary and show that the system exhibits some interesting behaviour as described below.

Recall from section 5, that for $\tau = 1$ the system exhibits stable phase-locked oscillations when the trivial solution loses stability, whereas when $\tau = 2.8$ it exhibits synchronous oscillations. Based on our analytical results and numerical continuations, we postulate that this behaviour persists in some region close to the stability region of the trivial solution. Thus we see that by changing the delay, we can change the type of oscillation exhibited by the system. Figure 5 illustrates this even more dramatically: for a range of values of $\beta$ we can observe several switchings between the two types of oscillations as the delay is increased. This is reminiscent of the delay induced switching between stability and oscillations observed in a scalar two delay model [2] and a second order, single delay model [9].

Note from figures 2 and 5 that intersections between the various curves of Hopf and pitchfork bifurcations can occur. Such points correspond to co-dimension two bifurcation points or points of bifurcation interaction. A complete discussion of these points is beyond the scope of this paper (see [3]); however, we note that with the choice of nonlinearities made above ($f(u) = \tanh(u)$, $g(u) = (1/\gamma)\tanh(\gamma u)$) most of the bifurcation interactions occur when the two bifurcations are supercritical. It is thus possible that in the neighbourhood of

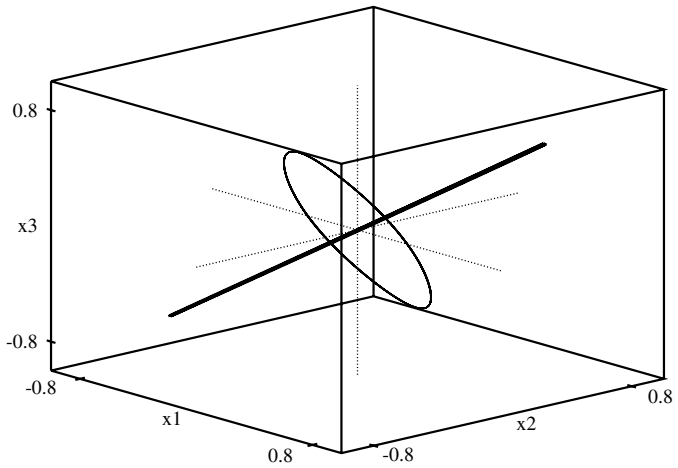


**Figure 6.** Numerical simulations of equation (1) with $n = 3, \alpha = 1.5, \tau_s = 1, \beta = 1, \tau = 1.8, \gamma = 1$.

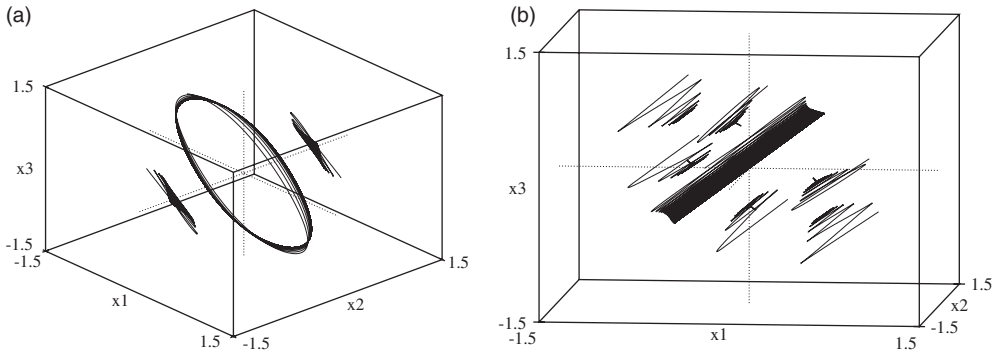


$\tau = 1, \beta = 1.3$ $\tau = 0.4, \beta = -2.6$

**Figure 7.** Numerical simulations of (1) with $n = 3, \alpha = 1.5, \tau_s = 1, \gamma = 1$ and other parameter values as shown.

such points one should find regions of multistability [15, sections 7.4–7.5]. In fact we do, as illustrated in figures 6 and 7. Figure 6 shows the coexistence of a stable synchronous periodic solution (i.e. one with $x_1(t) = x_2(t) = x_3(t)$) with one of the two stable phase-locked periodic solutions. This is the result of the standard Hopf/equivariant Hopf interaction point at $n = 3, \alpha = -1.5, \tau_s = 1, \beta \approx 0.883, \tau \approx 1.78$ (see figure 2). Such multistability is also observed numerically in the regions (indicated with a letter B) close to Hopf/Hopf interaction points in figure 5. Figure 7(*a*) shows the coexistence of a pair of stable synchronous equilibria with one of the two stable phase-locked periodic solutions. This is the result of the standard pitchfork/equivariant Hopf interaction point at $n = 3, \alpha = -1.5, \tau_s = 1, \beta = 1.25, \tau \approx 0.661$ (see figure 2). Figure 7(*b*) shows the coexistence of six stable equilibria with a stable synchronous periodic solution. This is the result of the standard Hopf/equivariant pitchfork interaction point at $n = 3, \alpha = -1.5, \tau_s = 1, \beta = -2.5, \tau \approx 0.397$ (see figure 2). These numerical simulations were performed using a fourth order Runge–Kutta solver adapted for delay differential equations, available through the package XPPAUT [11].

Both the phenomena described above arise because the Hopf bifurcation curves in figures 2 and 5 are nonmonotone. It was shown in [31] that this occurs if $\tau_s > |\alpha|/(|\alpha|^2+\sqrt{1+|\alpha|})$. Thus the nonmonotonicity is possible because system (1) has two delays. Nonmonotonic bifurcation curves are not possible in the corresponding system with one delay studied by [16, 30], and thus we would not expect to find multistability or delay induced switching between different oscillation types in those systems.

We have shown that for the equivariant bifurcations in our system there are only two possibilities: all branches of periodic solutions are supercritical or all are subcritical. In fact these are not the only possible situations for Hopf bifurcation with $\boldsymbol{D}_n$ symmetry. As discussed in [12, chapter XVIII], there are two other cases where some of the branches are supercritical and others are subcritical. In our case, these do not occur due to restrictions on the coefficients of the normal form (cf equations (48) and (49)). We suspect that if we relax the restriction $f''(0) = g''(0) = 0$ on our nonlinearities then we might be able to observe these other behaviours [4].

To close we note that our theoretical predictions could be verified experimentally. Marcus and Westervelt [23] constructed an electric circuit neural network where each element consists of a resistor and a capacitor and the elements are connected with nonlinear, delayed amplifiers. They show that this circuit is quite accurately represented by the model

$$C\dot{u}_i(t) = -\frac{u_i}{R} + \sum_{j=1}^{n} T_{ij}\tanh(Bu_i(t-\tau)), \qquad i = 1,\ldots,n.$$

They studied circuits with $C = 10\,\mathrm{nF}$, $R = 100\,\mathrm{k\Omega}$, $T_{ij} = T_{ji} \in \{-1/R, 0, 1/R\}$, $T_{ii} = 0$, $n = 2,\ldots,8$, were able to achieve delays over the range 0.4–8 RC and to adjust the gain on the amplifier in the range 3–20 $\mathrm{V}^{-1}$ [24, figure 3]. Clearly, if $T_{ij} = T$ and time is rescaled via $t \to (1/\mathrm{RC})t$ then this model corresponds to our model (1) with $\alpha = 0$, $\beta = RTB$, $\gamma = B$. Thus the range of delay and gain values does cover a large portion of the range of values included in figures 2 and 5. Assuming that a self-connection with a nonlinear, delayed amplifier could be added to each element, it should be possible to observe the phenomena we describe above in this experimental system. For example, one could vary the delay while holding the other parameters fixed to see if the observed solution switches type (between synchronous and phase-locked) as predicted by figure 5.

## Acknowledgments

SC and YY acknowledge the support of NSERC through the Discovery Grants Program. SB acknowledges the support of NSERC through the PDF Program.

## References

[1] Baldi P and Atiya A F 1994 How delays affect neural dynamics and learning *IEEE Trans. Neural Networks* **5** 612–21

[2] Bélair J and Campbell S A 1994 Stability and bifurcations of equilibria in a multiple-delayed differential equation *SIAM J. Appl. Math.* **54** 1402–24

[3] Bungay S D, Campbell S A and Yuan Y 2005 Patterns of oscillations in a ring of identical cells with delayed coupling, in preparation

[4] Buono P and Bélair J 2003 Restrictions and unfolding of double Hopf bifurcation in functional differential equations *J. Diff. Eqns* **189** 234–66

[5] Campbell S A 1999 Stability and bifurcation of a simple neural network with multiple time delays *Differential Equations with Application to Biology* ed S Ruan *et al* (*Fields Institute Communications* vol 21) (Providence, RI: American Mathematical Society) pp 65–79

[6] Campbell S A, Ncube I and Wu J 2004 Multistability and stable asynchronous periodic oscillations in a multiple-delayed neural system *Preprint*
[7] Campbell S A, Ruan S and Wei J 1999 Qualitative analysis of a neural network model with multiple time delays *Int. J. Bifurcat. Chaos* **9** 1585–95
[8] Cohen M and Grossberg S 1983 Absolute stability of global pattern formation and parallel memory storage by competitive neural networks *IEEE Trans. Syst. Man Cybernet.* **13** 815–26
[9] Cooke K L and Grossman Z 1982 Discrete delay, distributed delay and stability switches *J. Math. Anal. Appl.* **86** 592–627
[10] Engelborghs K, Luzyanina T and Samaey G 2001 DDE-BIFTOOL v. 2.00: a Matlab package for bifurcation analysis of delay differential equations *Technical Report* TW-330, Department of Computer Science, K U Leuven, Leuven, Belgium
[11] Ermentrout B 2002 *Simulating, Analyzing, and Animating Dynamical Systems: A Guide to XPPAUT for Researchers and Students* (Philadelphia, PA: SIAM)
[12] Golubitsky M, Stewart I and Schaeffer D G 1988 *Singularities and Groups in Bifurcation Theory* vol II (New York: Springer)
[13] Grossberg S 1978 Competition, decision, and consensus *J. Math. Anal. Appl.* **66** 470–93
[14] Grossberg S 1980 Biological competition: decision rules, pattern formation, and oscillations *Proc. Natl Acad. Sci. USA* **77** 2338–42
[15] Guckenheimer J and Holmes P J 1983 *Nonlinear Oscillations, Dynamical Systems and Bifurcations of Vector Fields* (New York: Springer)
[16] Guo S and Huang L 2003 Hopf bifurcating periodic orbits in a ring of neurons with delays *Physica* D **183** 19–44
[17] Hale J K and Verduyn Lunel S M 1993 *Introduction to Functional Differential Equations* (New York: Springer)
[18] Hopfield J J 1984 Neurons with graded response have collective computational properties like those of two-state neurons *Proc. Natl Acad. Sci. USA* **81** 3088–92
[19] Hopfield J J 1982 Neural networks and physical systems with emergent collective computational abilities *Proc. Natl Acad. Sci. USA* **79** 2554–8
[20] Krawcewicz W, Vivi P and Wu J 1997 Computation formulae of an equivariant degree with applications to symmetric bifurcations *Nonlinear Studies* **4** 89–119
[21] Krawcewicz W and Wu J 1999 Theory and applications of Hopf bifurcations in symmetric functional-differential equations *Nonlinear Anal.* **35** 845–70
[22] Marcus C M, Waugh F R and Westervelt R M 1991 Nonlinear dynamics and stability of analog neural networks *Physica* D **51** 234–47
[23] Marcus C M and Westervelt R M 1988 Basins of attraction for electronic neural networks *Neural Information Processing Systems* (*Denver, CO, 1987*) ed D S Anderson (New York: AIP) pp 524–33
[24] Marcus C M and Westervelt R M 1989 Stability of analog neural networks with delay *Phys. Rev.* A **39** 347–59
[25] Ncube I, Campbell S A and Wu J 2003 Change in criticality of synchronous Hopf bifurcation in a multiple-delayed neural system *Dynamical Systems and their Applications to Biology* ed S Ruan *et al* (*Fields Institute Communications* vol 36) (Providence, RI: American Mathematical Society) pp 179–93
[26] Orosz G and Stépán G 2004 Hopf bifurcation calculations in delayed systems with translational symmetry *J. Nonlinear Sci.* **14** 505–28
[27] Orosz G, Wilson R E and Krauskopf B 2004 Global bifurcation investigation of an optimal velocity traffic model with driver reaction time *Phys. Rev.* E **70** 026207
[28] Shayer L P and Campbell S A 2000 Stability, bifurcation and multistability in a system of two coupled neurons with multiple time delays *SIAM J. Appl. Math.* **61** 673–700
[29] Wu J 1998 Symmetric functional-differential equations and neural networks with memory *Trans. Am. Math. Soc.* **350** 4799–838
[30] Wu J, Faria T and Huang Y S 1999 Synchronization and stable phase-locking in a network of neurons with memory *Math. Comput. Modelling* **30** 117–38
[31] Yuan Y and Campbell S A 2004 Stability and synchronization of a ring of identical cells with delayed coupling *J. Dyn. Diff. Eqns* **16** 709–44